# The employ of manganese oxide to improve the selectivity of gas sensitive $SnO_x$ films

© V.V. Bolotov, E.V. Knyazev, K.E. Ivlev¶, I.V. Ponomareva, Yu.A. Sten'kin, S.N. Nesov, E.A. Roslikova

Omsk Scientific Center, Siberian Branch, Russian Academy of Sciences,
644024 Omsk, Russia

¶ E-mail: 85konst85@gmail.com

*Received May 2, 2024*
*Revised August 5, 2024*
*Accepted November 14, 2024*

To improve the selectivity of gas-sensitive $SnO_x$ films, $SnO_x/MnO_y$ composite structures were obtained in which manganese oxide plays the role of a $NO_2$ sorbing filter. The microstructure and chemical composition of the films were characterized using scanning electron microscopy and X-ray photoelectron spectroscopy. The structures were tested to detect 5 ppm $NO_2$ at room temperature. The sensory response of $SnO_x$ films in the presence of $NO_2$ decreases by 16 times after coating the $MnO_y$ filter layer.

**Keywords:** filters, microsensors, manganese oxide, tin dioxide.

DOI: 10.61011/SC.2024.09.59913.6438A

The task of obtaining interconnected multilevel structures on porous media with layers of various morphologies obtained in a single technological process and their subsequent functionalization is of great interest in micro- and nanosensorics. In particular, it is possible to create a vertically integrated sensor structure, including transport layers for the analyte gas, filtering layers, sorbing and sensitive layers.

Given the low cost and miniaturization of microsensors compared to gas analyzers and the possibility of using sensor networks to multiply information, chemical microsensors may represent a cheaper alternative for detecting gases. Microsensors are based on physico-chemical principles and are usually sensitive enough for most applications, but their low selectivity is a major limitation for the selective detection of a single component. The use of nonstoichiometric tin dioxide films as a sensing element is limited by their selectivity and stability as a result of morphological changes in the sensing material (grain growth) or chemical irreversible reactions with a number of gases. Active filters can be used to improve the selectivity of $SnO_x$ films. $SnO_x$ films are easily applied to porous silicon substrates by various methods, which makes it possible to create a vertically integrated sensor structure. A number of papers [1,2] show that $MnO_2$ layers can be used as filters for $SnO_x$ and $WO_3$ films, in particular for ozone. Nanomaterials based on manganese oxide in various polymorphic modifications and degrees of oxidation are used as sensitive elements for detecting mainly reducing gases, such as $H_2$, $NH_3$, $C_2H_4$, $With_2H_5OH$, $CH_3CN$, CO. As a rule, the sizes of manganese oxide nanoparticles for sensitive elements are 20−200 nm [3–8]. For $MnO_2$ used as active filters, the particle sizes were on the order of units of micrometers [2].

The development of film technologies for applying functional layers is the most important for the integration and creation of multi-sensor devices. This paper shows the possibility of obtaining filters based on $MnO_y$ as a nitrogen dioxide sorbent applied to $SnO_x$ films.

$MnO_y$ layers were obtained by thermal decomposition of manganese nitrate in ethyl alcohol and deposited on pre-formed $SnO_x$ films on citallic and silicon substrates. $SnO_x$ was obtained by chemical vapor-phase deposition [9]. A layer of $Mn(NO_3)_2$ solution in 0.14 M ethyl alcohol was first applied to the substrates. The samples were then dried at room temperature. Then the substrates were slowly heated to a temperature of 350°C, and kept at this temperature for 5 min. Next, the samples were cooled to room temperature, and the manganese nitrate solution was applied in layers again in the same mode until a sufficiently noticeable and durable layer of $MnO_y$ was formed.

The morphology and elemental composition of $SnO_x/MnO_y$ structures were studied using scanning electron microscopy (SEM) and energy dispersion analysis (EDA) using Jeol JSM-6610-LV scanning electron microscope with an energy dispersion analyzer Inca-XAct. The SEM images of $SnO_x/MnO_y$ samples obtained in the secondary electron registration mode show a $SnO_x$ layer having a granular structure with a grain size of $\sim 100$ nm, which is partially covered by a layer manganese oxide. The grain size of the manganese oxide layer varies in the range of $0.5-2\,\mu$m. According to EDA data, the concentration of manganese is 0.2 at% in the areas where the granular structure is observed (Figure 1, point *1*), while this value is 3.4 and 1.9 at%, respectively, in the upper layer (Figure 1, points *2* and *3*). The tin concentration at these points is 5.5, 4.0, and 4.9 at%, respectively. Lighter contrast at points *2* and *3* compared to point *1* is explained by the high resistivity of manganese oxide compared to the resistivity of tin oxide.

The chemical composition of the surface of $MnO_y$ layers deposited on $SnO_x$ films stained with Si by X-ray photoelectron spectroscopy (XPS) was studied. Figure 2

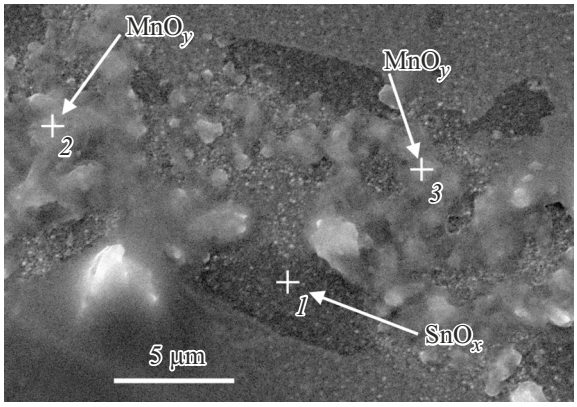


**Figure 1.** REM image of $SnO_x/MnO_y$ layer. Crosses mark the points where the elemental composition was analyzed using the EDA method.

shows an overview of the XPS spectrum of $SnO_x/MnO_y$ sample before and after exposure in $NO_2$ pairs. The spectrum of the initial sample contains photoelectron lines of manganese (Mn $2p$, Mn $3s$), oxygen (O $1s$), tin (Sn $3d$) and carbon (C $1s$). The presence of carbon is associated with the adsorption of pollutants during the storage of the sample in the air. Exposure to an atmosphere saturated with nitrogen dioxide slightly changes the appearance of the viewing spectrum. A nitrogen line (N $1s$) is detected in the spectrum, indicating sorption of $NO_2$ on the surface of $SnO_x/MnO_y$ sample. Also, a change of the shape of the manganese peak (Mn $2p$) is visible on the overview XPS spectrum. The shape of Mn $2p$ peak on the spectrum before exposure in $NO_2$ has 2 maxima, which correspond to Mn $2p_{1/2}$ and Mn $2p_{3/2}$ lines [10]. In this case, the Mn $2p_{3/2}$ line has a higher intensity than Mn $2p_{1/2}$ line. This type of spectrum is typical for slightly oxidized manganese. Exposure to a saturated atmosphere $NO_2$ leads to an equalization of the intensities of Mn $2p_{1/2}$ and Mn $2p_{3/2}$ components, which is a sign of manganese oxidation. The analysis of the core Mn $3s$ spectrum also confirms this assumption. Mn $3s$ XPS of spectrum of the initial $SnO_x/MnO_y$ sample has 2 components with bond energies of 89.6 eV and 83.5 eV. The energy distance between the maxima of Mn $3s$ XPS of the spectrum of the initial sample is 6.1 eV, which corresponds to the state of MnO. Exposure to $NO_2$ atmosphere leads to a shift of the maximum of the low-energy component to 84.2 eV and a decrease of the energy distance between the maxima to 5.4 eV, which corresponds to higher degrees of oxidation of $Mn_2O_3-MnO_2$ [11].

The following table shows the results of quantitative elemental analysis carried out using the review XPS spectra of $SnO_x/MnO_y$ sample using elemental sensitivity coefficients. The analysis results show an increase of nitrogen concentration to 7.6 at% on the sample surface after exposure to $NO_2$ vapors, which also indicates sorption of nitrogen dioxide molecules by manganese oxide.

Studies of gas sensitivity at 5 ppm of $NO_2$ were conducted at room temperature. $SnO_x$ film on a citall substrate was used as a gas-sensitive element.

The response of a resistive gas-sensitive element was compared before and after application of the $MnO_y$ sorbing layer. The resistance of the resistive gas-sensitive element was estimated from linear volt-ampere characteristics, which were measured using an Agilent E4980A LCR meter. The response $S$ of the sensor element was calculated as $S = [(R_g - R_0)/R_0] \cdot 100\%$, where $R_g$ — the resistance of the element after exposure to gas, $R_0$ — the initial resistance of the element before exposure to gas.

The results of gas sensitivity testing are shown in Figure 3, *a*. The sensor response at an exposure to 5 ppm of $NO_2$ for $SnO_x$ films before application of the film sorbent

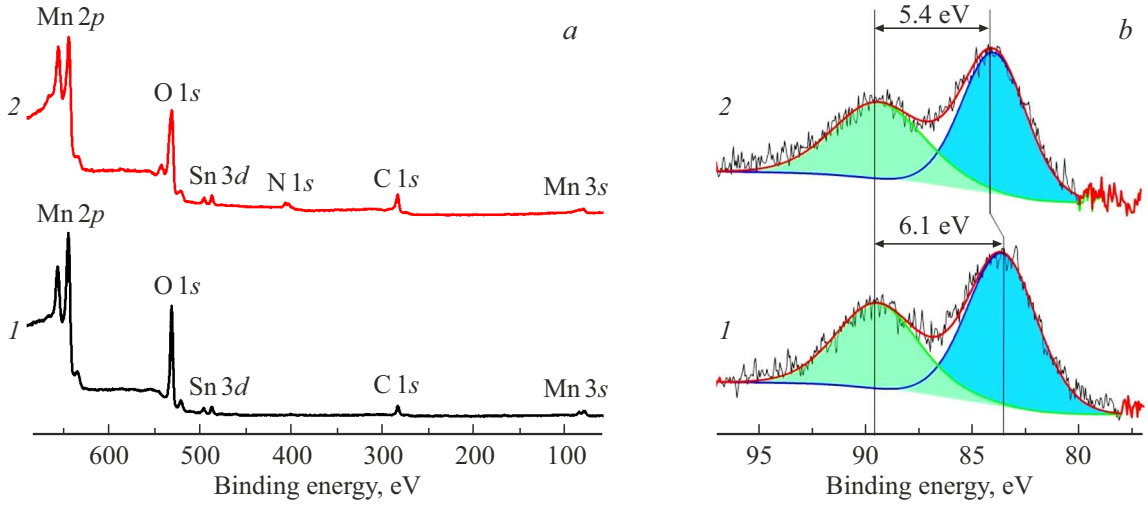


**Figure 2.** XPS spectra of $SnO_x/MnO_y$ sample: *a* — overview spectrum; *b* — Mn $3s$; *1* — spectrum of the initial sample, *2* — spectrum of the sample after exposure in $NO_2$.

Chemical composition of $SnO_x/MnO_y$ sample before and after exposure to $NO_2^*$ vapors

| Sample | [Mn] | [C] | [N] | [Sn] | [O] |
|---|---|---|---|---|---|
| $SnO_x/MnO_y$ | 22 | 24.5 | – | 0.5 | 53 |
| $SnO_x/MnO_y$ after $NO_2$ | 20 | 21.3 | 7.6 | 0.9 | 50.2 |

*Note.* * All results are in atom per cent.

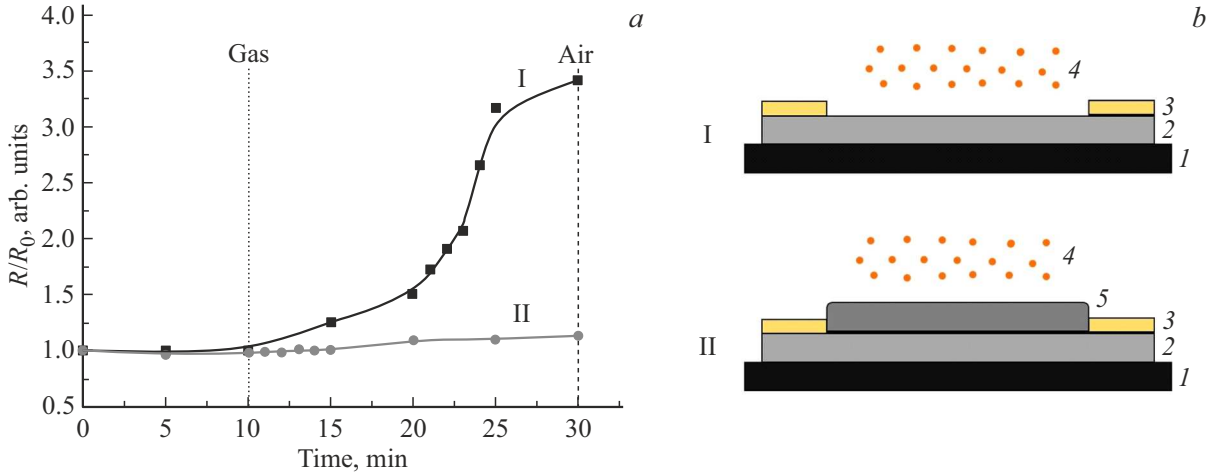


**Figure 3.** Change of the ratio of the resistance of the gas-sensitive element to the initial resistance at exposure to 5 ppm of $NO_2$ (*a*) and the schemes of the test structures (*b*): I — $SnO_x$, II — $SnO_x/MnO_y$; *1* — substrate, *2* — $SnO_x$ layer, *3* — metal contacts, *4* — $NO_2$ molecules, *5* — $MnO_y$ layer.

was 240%, it was 15% after application of the film sorbent. Comparing the results of electrophysical measurements with the XPS data, it can be said that the sorption of $NO_2$ molecules is accompanied by the oxidation of MnO to $Mn_2O_3$ and $MnO_2$.

The SEM data indicate that the surface of the sensor element ($SnO_x$) is partially covered with a layer of manganese oxide. According to the literature data in Ref. [1,2], this layer configuration makes it possible to efficiently sorb molecules of oxidizing gases. The obtained results of electrophysical studies indicate the absorption of nitrogen dioxide by the $MnO_y$ film. Studies of the surface of the $MnO_y$ layer before and after exposure in $NO_2$ vapors showed a change of the chemical state of manganese. A shift of the XPS components of the Mn, 3*s* spectrum is observed, which indicates the oxidation of the manganese layer. At the same time, quantitative elemental analysis indicates an increase of nitrogen concentration in the surface layers of the $SnO_x/MnO_y$ structure. The results obtained allow making a conclusion that the interaction of $NO_2$ vapors and the $MnO_y$ layer results in effective sorption of nitrogen dioxide molecules, which is accompanied by oxidation of the near-surface layers of $MnO_y$.

## Funding

The work has been performed under the state assignment from Omsk Scientific Center of the Siberian Branch of RAS (project state registration number 121021600004-7).

## Conflict of interest

The authors declare that they have no conflict of interest.

## References

[1] C. Pijolat, B. Riviere, M. Kamionka, J.P. Viricelle, P. Breuil. J. Mater. Sci., **38**, 4333 (2003). DOI: 10.1023/A:1026387100072
[2] Ch. Zhang, A. Boudiba, C. Navio, M.-G. Olivier, R. Snyders, M. Debliquy. Sensors Actuators B, **161**, 914 (2012). DOI: 10.1016/j.snb.2011.11.062
[3] L. Bigiani, D. Zappa, Ch. Maccato, E. Comini, D. Barreca, A. Gasparotto. Appl. Surf. Sci., **512**, 145667 (2020). DOI: 10.1016/j.apsusc.2020.145667
[4] D. Barreca, A. Gasparotto, F. Gri, E. Comini, Ch. Maccato. Adv. Mater. Interfaces, **5**, 1800792 (2018). DOI: 10.1002/admi.201800792
[5] L. Bigiani, D. Zappa, Ch. Maccato, A. Gasparotto, C. Sada, E. Comini, D. Barreca. Adv. Mater. Interfaces, **6**, 1901239 (2019). DOI: 10.1002/admi.201901239
[6] L. Bigiani, D. Zappa, Ch. Maccato, A. Gasparotto, C. Sada, E. Comini, D. Barreca. Nanomaterials, **10**, 511 (2020). DOI: 10.3390/nano10030511
[7] X.Q. Tian, L. Yang, X.X. Qing, K. Yu, X.F. Wang. Sensors Actuators B, **207**, 34 (2015). DOI: 10.1016/j.snb.2014.08.018
[8] C. Liu, S.T. Navale, Z.B. Yang, M. Galluzzi, V.B. Patil, P.J. Cao, R.S. Mane, F.J. Stadler. J. Alloys Compd., **727**, 362 (2017). DOI: 10.1016/j.jallcom.2017.08.150

[9] V.V. Bolotov, P.M. Korusenko, S.N. Nesov, S.N. Povoroznyuk, V.E. Roslikov, E.A. Kurdyukova, Yu.A. Sten'kin, R.V. Shelyagin, E.V. Knyazev, V.E. Kan, I.V. Ponomareva. Mater. Sci. Eng. B, **177**, 1 (2012). DOI: 10.1016/j.mseb.2011.09.006
[10] V. Mishra, B.D. Mohapatra, T.K. Ghosh, G.R. Rao. Electrocatalysis, **14**, 788 (2023). DOI: 10.1007/s12678-023-00836-9
[11] A.D. Fedorenko, L.N. Mazalov, E.Yu. Fursova, V.I. Ovcharenko, A.V. Kalinkin, S.A. Lavrukhina. J. Struct. Chem., **58** (6), 1166 (2017). DOI: 10.1134/S0022476617060142

*Translated by A.Akhtyamov*